お茶の水女子大学自然科学報告　第73巻　第1号、第2号
Natural Science Report, Ochanomizu University, Vol. 73, No. 1, No. 2 (2023)

Numerical simulation of the flow around four Savonius turbines

Akiko MINAKAWA and Tetuya KAWAMURA

(Received : August 31, 2022)

Abstract

One of the vertical axis wind turbines that utilize drag force is the Savonius turbine. Savonius turbines are characterized by low speed rotation and high torque, so they are rarely used for wind power generation but have possibility to apply to ocean current power generation, which has been attracting attention recently. In this report, we actually performed a numerical simulation of the flow using suitable grid, focusing mainly on the case where four wind turbines are rotating in reverse at a constant speed, and investigated the state of the flow field. Two-dimensional incompressible Navier-Stokes equations are adopted as the basic equation and solved numerically using the finite difference method. In addition, in order to enable calculation even in a high Reynolds number flow, the nonlinear term of the equations are approximated by using the third-order accuracy upstream difference method. The simulations are performed with 0 degrees flow and 45 degrees flow for four turbines position. The flow field differs greatly depending on each angle, and the interaction between the wind turbines has been clarified.

1. INTRODUCTION

Fossil fuels account for most of the world's energy production, but there is a need to reduce the burden on the environment. Therefore, utilization of renewable energy is important. Ocean current power generation is an energy acquisition method that is expected to develop in the future. For large-scale wind power generation, horizontal axis type rotating devices such as propellers have been put into practical use. On the other hand, the technology for ocean current power generation is under development for practical use, and the optimum shape of the rotating device has not been determined. Focusing on the fact that the ocean current has a slower flow velocity than the wind, it is considered that a sufficient amount of power generation can be obtained by arranging a plurality of drag-type vertical axis-type rotating devices. Savonius turbine is one of the vertical axis type rotators using drag force. It has the potential to be used for ocean current power generation because of its low rotational speed and high torque output. If it is installed in the sea, it will be improved the stability of the whole device to connect the two turbines with a support rod and rotated in opposite directions. In that case, it is necessary to install the two turbines close to each other to make the entire ocean current power generation device smaller, and the interaction between the turbines cannot be ignored. The interaction between the two turbines is reported by experiments[1], varying the distance between the turbines or the direction of the mainstream. It was found that arranging Savonius turbines in close proximity to a specific range of angles can improve power output by up to 112% for a single turbine. A numerical simulation study[2] also showed that installation at a particular angle improved the output. In this study, two-dimensional numerical simulations were performed with a fixed rotation speed for four Savonius turbines rotating in opposite directions independently. The effect on the flow and torque was investigated by changing the angle of attack and the rotational speed independently.

2. MODELS AND GRID GENERATION

2.1 Models

In this study, as shown in Fig.1, we assume the case of arranging four same-sized Savonius turbines that rotate independently in opposite directions at constant angular velocities. The line connecting the rotation axes of the device is taken as the x-axis and the y-axis. It is assumed that the flow is in two directions, the angles with the x-axis set to 0 degrees and 45 degrees.

2.2 Division of Computational Domain

In general, when analyzing a flow around a rotating object, a rotating coordinate system that rotates with the same rotating speed of the object is often used[3][4].However, when multiple objects rotate, how to set the rotating coordinate system becomes a problem. In this study, in order to make it possible to calculate four Savonius turbines individually, four regions including one turbine are connected together as an overall computational domain (Fig.2). As shown in Fig.3, each device region is roughly divided into a static coordinate system region (Fig.3 left) and a rotating coordinate system region (Fig.3 right). The region of the stationary coordinate system is divided into an external region A and a connected region B that touches the rotating region. The boundary where the non-rotating region B and the rotating region C meet is a circular ring. The ring part is overlapped by one grid, and data is passed between regions. As a result, it is possible to improve the accuracy of the interpolation of physical quantities in the two regions. In addition, the region of the rotating coordinate system of each device is divided into the rotating region C around the blade, the inflow/outflow region D inside the blade, and the blade overlapping region E. Then, data is transferred by matching the grids at the boundaries of each region. As a result, it became possible to analyze the flow inside and outside the blade.

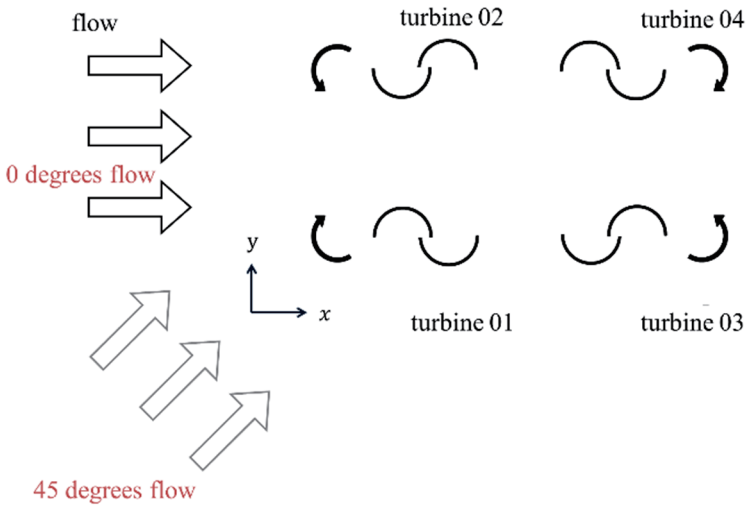

Fig.1 Schematic diagram of four Savonius turbines

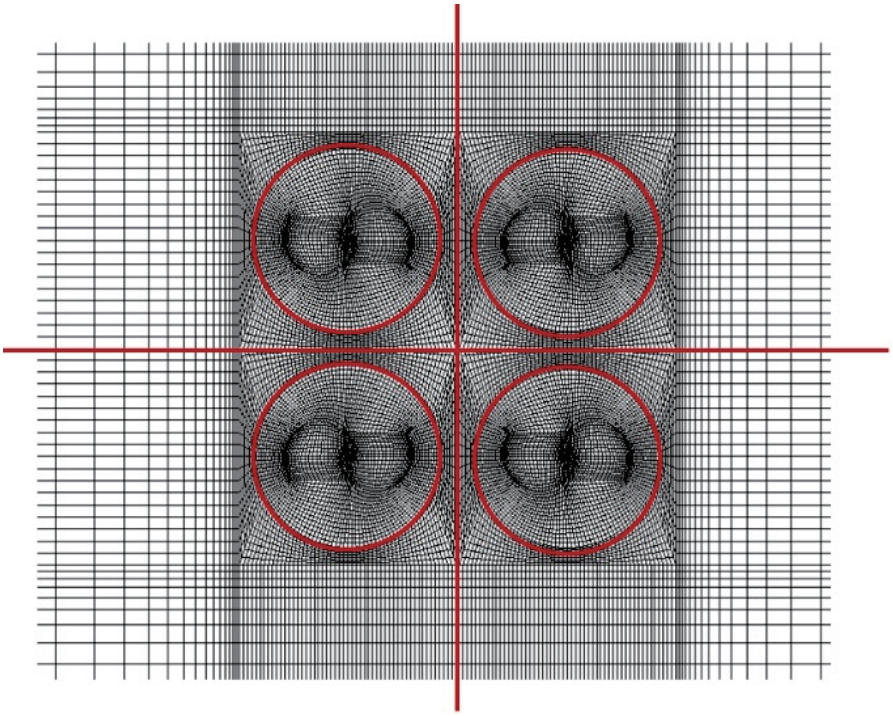

Fig.2 Computational grid for four turbines

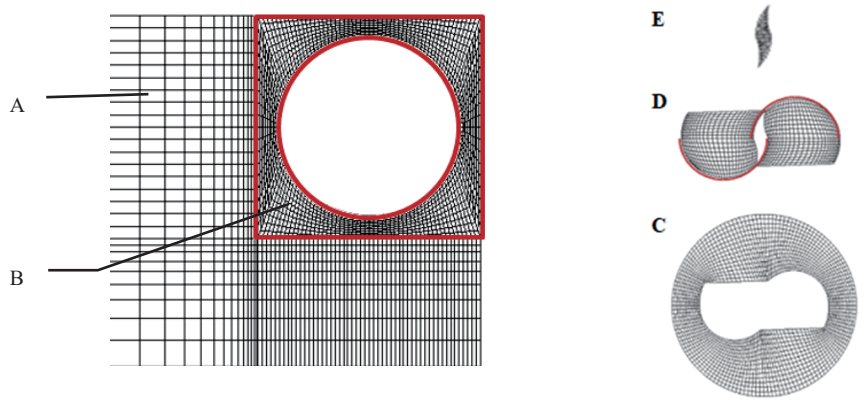

Fig.3 Stationary coordinate system grid (left) and rotating coordinate system grid (right)

3. NUMERICAL METHODS

3.1 Basic equations

In the rotating region near the rotating device, a rotating coordinate system fixed to the rotating device is used. As shown in Fig.4, the relationship between the position (X, Y) in the rotating coordinate system and the position (x, y) in the stationary coordinate system can be expressed as follows where θ (=ωt, ω: angular velocity) is the rotation angle measured from the stationary state.

$$X = x\cos\theta - y\sin\theta \quad (1)$$

$$Y = x\sin\theta + y\cos\theta \quad (2)$$

Similarly, the relationship between the velocity (U, V) in the rotating coordinate system and the velocity (u, v) in the stationary coordinate system can be expressed by the following equation.

$$U = u\cos\theta - v\sin\theta - \omega Y \tag{3}$$
$$V = u\sin\theta + v\cos\theta + \omega X \tag{4}$$

Fig.4: Coordinate systems

Continuity equations and Navier-Stokes equations in stationary and rotating coordinate systems are used as basic equations. Two-dimensional continuity equations and incompressible Navier-Stokes equations expressed in stationary and rotating coordinates are as follows.

$$\frac{\partial u}{\partial x} + \frac{\partial v}{\partial y} = 0 \tag{5}$$
$$\frac{\partial u}{\partial t} + u\frac{\partial u}{\partial x} + v\frac{\partial u}{\partial y} = -\frac{\partial p}{\partial x} + \frac{1}{Re}\left(\frac{\partial^2 u}{\partial x^2} + \frac{\partial^2 u}{\partial y^2}\right) \tag{6}$$
$$\frac{\partial v}{\partial t} + u\frac{\partial v}{\partial x} + v\frac{\partial v}{\partial y} = -\frac{\partial p}{\partial y} + \frac{1}{Re}\left(\frac{\partial^2 v}{\partial x^2} + \frac{\partial^2 v}{\partial y^2}\right) \tag{7}$$
$$\frac{\partial U}{\partial X} + \frac{\partial V}{\partial Y} = 0 \tag{8}$$
$$\frac{\partial U}{\partial t} + U\frac{\partial U}{\partial X} + V\frac{\partial U}{\partial Y} - \omega^2 X + 2\omega V = -\frac{\partial p}{\partial X} + \frac{1}{Re}\left(\frac{\partial^2 U}{\partial X^2} + \frac{\partial^2 V}{\partial Y^2}\right) \tag{9}$$
$$\frac{\partial U}{\partial t} + U\frac{\partial V}{\partial X} + V\frac{\partial V}{\partial Y} - \omega^2 Y - 2\omega U = -\frac{\partial p}{\partial Y} + \frac{1}{Re}\left(\frac{\partial^2 V}{\partial X^2} + \frac{\partial^2 V}{\partial Y^2}\right) \tag{10}$$

Here p represents pressure. *Re* is the Reynolds number with the radius of the rotating device as the representative length and the flow velocity of mainstream as the representative velocity.

3.2 Numerical method

After transforming the above basic fluid equations into general coordinates, the fractional step method[5] is used to solve them. Third-order upstream differencing[6] is applied to the nonlinear terms (convective terms) of the Navier-Stokes equations, and central differencing is applied to others.

4. RESULTS AND DISCUSSIONS

4.1 Flow near the turbines

Following figures show the flow field in the vicinity of the turbines when the four turbines rotate at a tip speed ratio of λ=0.5. Fig.5 shows the results when the angle of attack of the flow is 0 degrees, that is, the flow comes from left to right in the figure. The velocity vectors at the time when the turbine rotates 45, 90, 135, and 180 degrees from one rotation after the start of rotation are shown in time series, and the black arrows in the figure represent the flow velocity vectors. Fig.6 shows contour lines representing the pressure values in the same case using the colors shown in the color bar in the figure. From Fig.5 and Fig.6, it can be seen that the flow and pressure distributions are roughly symmetrical around turbine01 and turbine03 in the lower half of the figures and around turbine02 and turbine04 in the upper half, with the line along the mainstream in the center of the computational domain as the axis of symmetry. Looking at the contour lines in Fig.6, it can be seen that the data is transferred well along the line of the divided regions.

It can be also seen that the pressure around turbine01 and turbine02 on the upstream side of the flow is higher than that around turbine03 and turbine04 on the downstream side.

Fig.7 shows the velocity vector when the angle of attack of the flow is 45 degrees, that is, the flow flows from the lower left to the upper right in the figure, and Fig.8 shows the pressure values in the same way as Fig.5 and Fig.6. Due to the rotation of turbine01 and turbine02, the flow is being drawn between the two turbines. At this time, a vortex is generated by changes in pressure and velocity as the flow passes through the narrow area between the turbines and flows out into the wider area (Fig.8(a)). Furthermore, due to the rotation of turbine02, it is drawn between turbine01 and turbine02, and after passing through the narrow area between the turbines, a vortex is generated in the flow again (Fig.8(c)). Regarding the mainstream flow, the flow rate between turbine01 and turbine03 is considered to be small compared to the flow rate between turbine01 and turbine02. This is due to the fact that the flow is pulled in between turbine01 and turbine02 as the turbines rotate, whereas the flow is pushed out from the inside to the outside of the region between turbine01 and turbine03 due to the rotation of the turbines, making it difficult for the mainstream to flow in.

From Fig.8, it can be seen that the pressure distribution tends to be symmetrical with respect to the line connecting the centers of turbine01 and turbine04. On the other hand, the positions where vortices are generated and-contour lines are not necessarily symmetrical. This is due to the direction of rotation of each turbine. Also, in Fig.8(a), the vortex generated by the flow drawn in due to the rotation of the turbine01 and turbine02 flows out to the rear of the turbine04. At that time, the vortex passes between the turbine02 and turbine04 as the turbine02 rotates (Fig.8(b)(c)). Based on the direction of rotation of each turbine, the route through which this vortex flowed out had the highest flow rate.

(a) θ=450 (b) θ=495

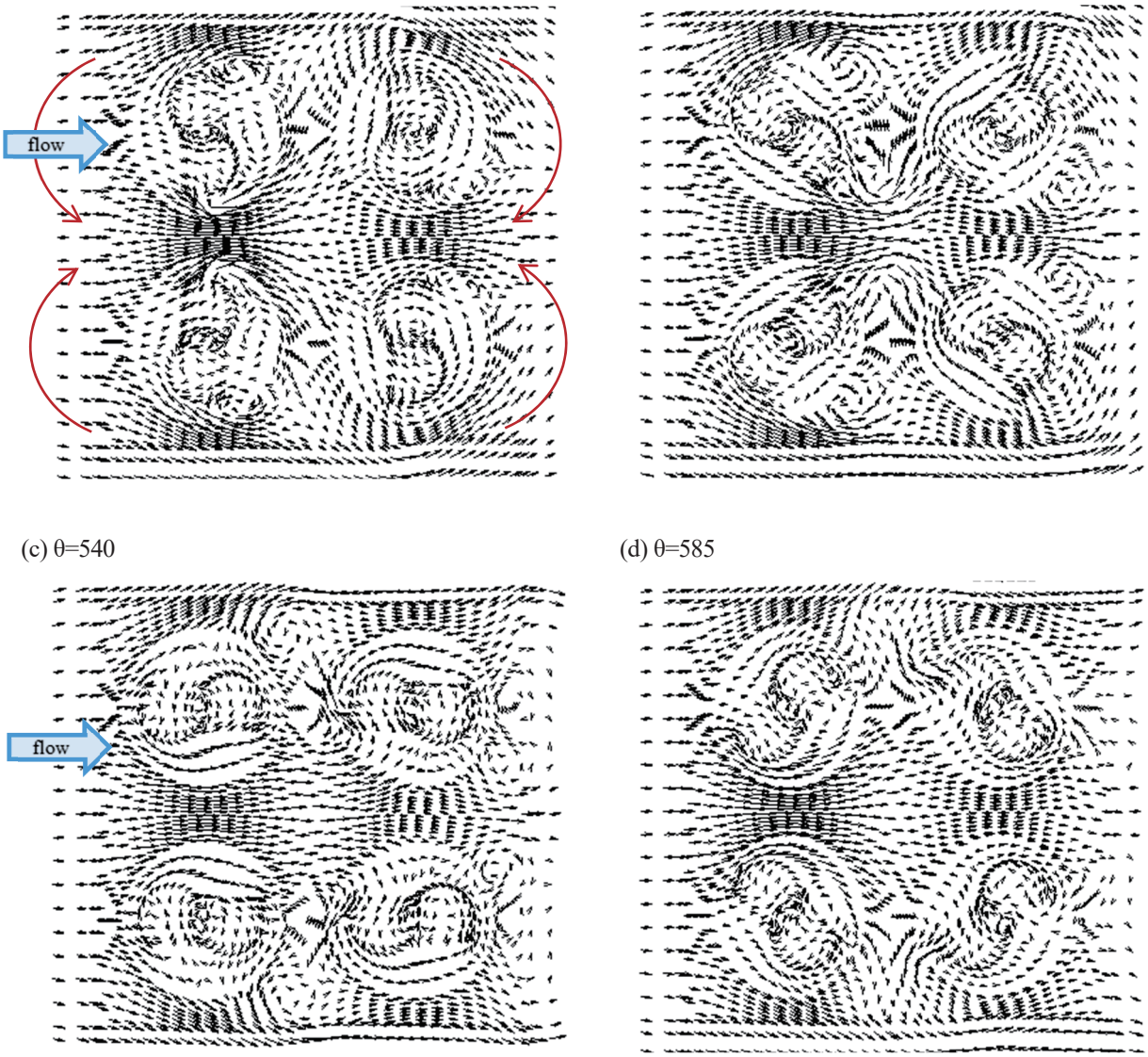

(c) θ=540 (d) θ=585

Fig.5: Velocity field (0 degrees flow)

(a) θ=450 (b) θ=495 (c) θ=540 (d) θ=585

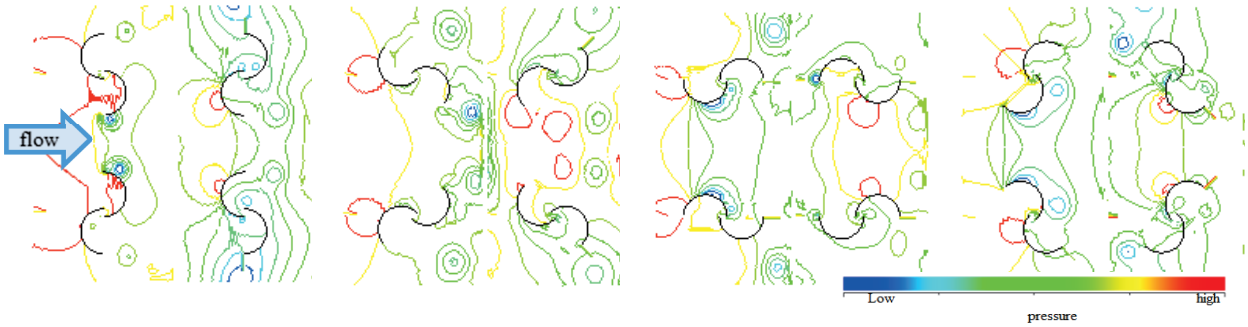

Fig.6: Contour line of pressure (0 degrees flow)

(a) θ=450 (b) θ=495

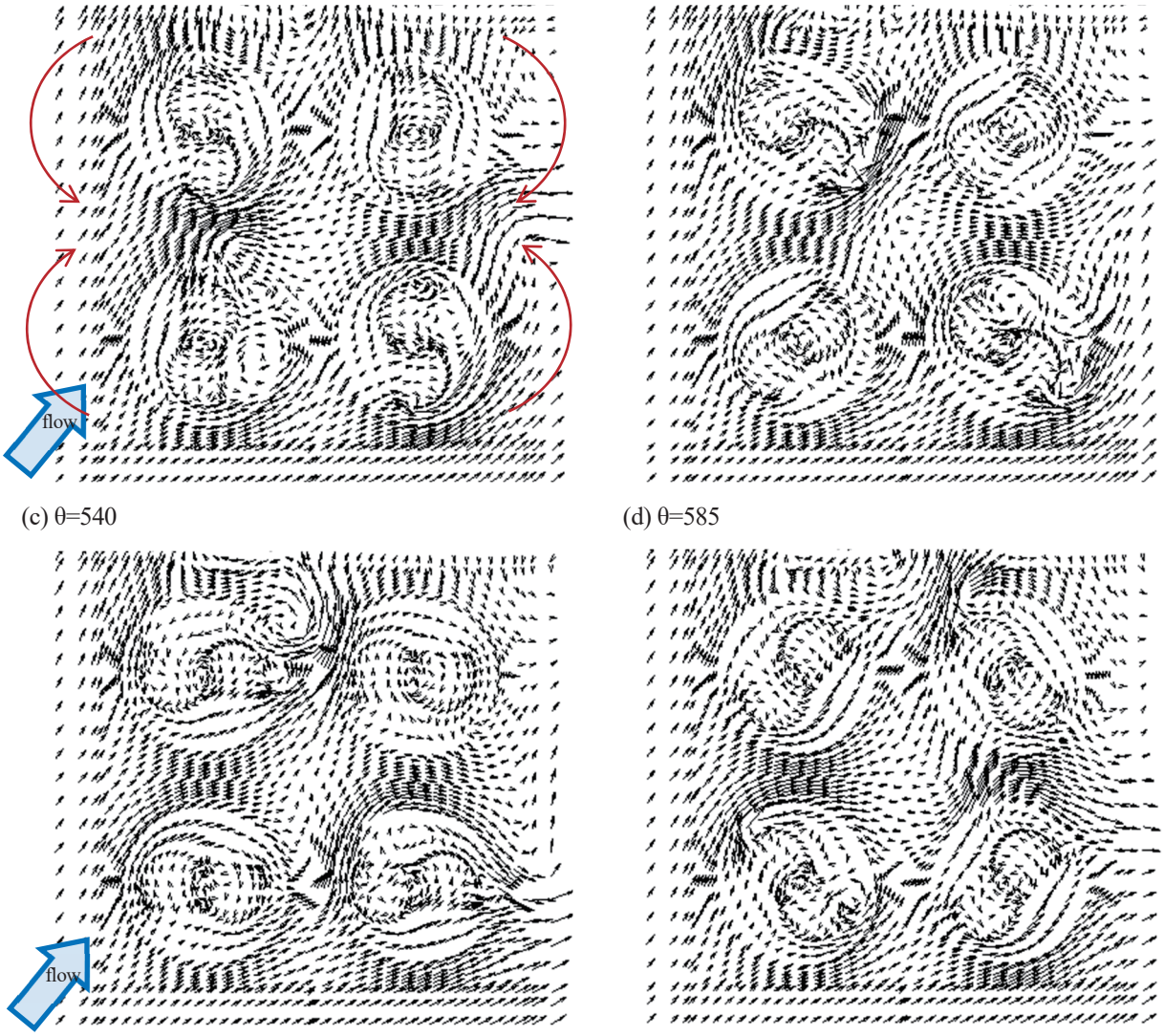

(c) θ=540 (d) θ=585

Fig.7: Velocity field (45 degrees flow)

(a) θ=450 (b) θ=495 (c) θ=540 (d) θ=585

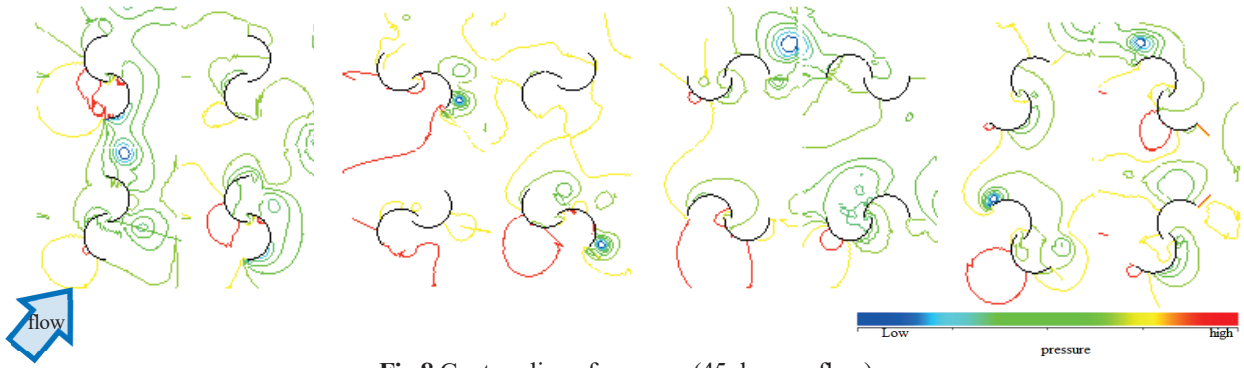

Fig.8 Contour line of pressure (45 degrees flow)

4.2 Torque coefficient

Following figures shows the torque coefficient when four turbines are rotated at a peripheral speed ratio of $\lambda = 0.5$. Fig.9 and Fig.10 show the time history of the torque coefficient of turbine01 when the mainstream is 0 degrees and 45 degrees. The horizontal axis represents the rotation angle, and the vertical axis represents the torque coefficient. In this figure, the torques of the two blades of the rotating device are plotted with red and blue dotted lines, and the total torque of the two blades is plotted with the solid line. The torque of each blade is 180 degrees out of phase with a 360 degrees cycle, but the values are about the same. The total torque value of the two blades (torque for one turbine) has two peaks in one cycle. In addition, there is a difference in the torque value between the 0 degrees flow and the 45 degrees flow. These are considered to be affected by differences in interaction with other turbines caused by the direction of the mainstream.

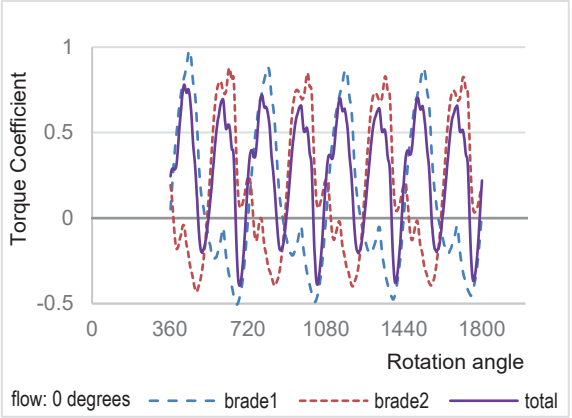

Fig.9 Time history of the torque coefficient (Turbine01, 0 degrees flow)

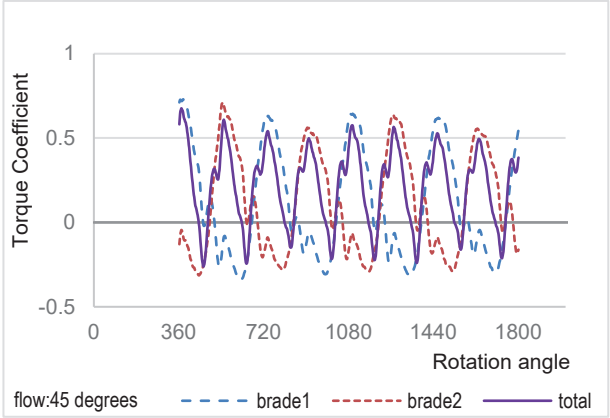

Fig.10 Time history of the torque coefficient (Turbine01, 45 degrees flow)

Fig.11 and Fig.12 show the time history in the torque of each of the four turbines when the mainstream is 0 degrees and 45 degrees. The layout of the graph corresponds to the layout in Fig.1. In Fig.11, it is seen that the torques of turbine01 and turbine02 located upstream, and turbine03 and turbine04 located downstream are approximately equal. The downstream turbine has a smaller torque value than the upstream turbine, and it is considered that this is because the upstream turbine does not receive the mainstream directly. In Fig.12, the torque values of turbine02 and turbine03 are larger than those of turbine01. It is thought that in the case of the flow from the 45 degrees direction, turbine02 and turbine03 can directly receive the mainstream without being blocked by other turbines while the torque increased due to the addition of the flow changed by the turbine01.

Fig.13 and Fig.14 show the temporal changes in the torque of each of the four turbines and the total torque of the four turbines when the mainstream is 0 degrees and 45 degrees. It is difficult to grasp and compare the total torque due to rotation because the total torque value of the four turbines changes in a complicated manner. Therefore, the values obtained by accumulating the torque over whole time are compared. Fig.15 shows the torque of each of the four turbines integrated over time. The layout of the graph corresponds to the layout in Fig.1, as in Fig.11 and Fig.12. Fig.16 shows the integrated torque of the four units. Comparing the individual torque integrated values, only turbine01 has a value greater than 45 degrees at mainstream 0 degrees, and the other turbines have values at 45 degrees mainstream greater than 0 degrees. The torque integrated value of the total of four turbines increased almost linearly with rotation. This means that stable output can be obtained with multiple turbines. In addition, when the mainstream is 45 degrees, the value is about 68% larger than when the mainstream is 0 degrees.

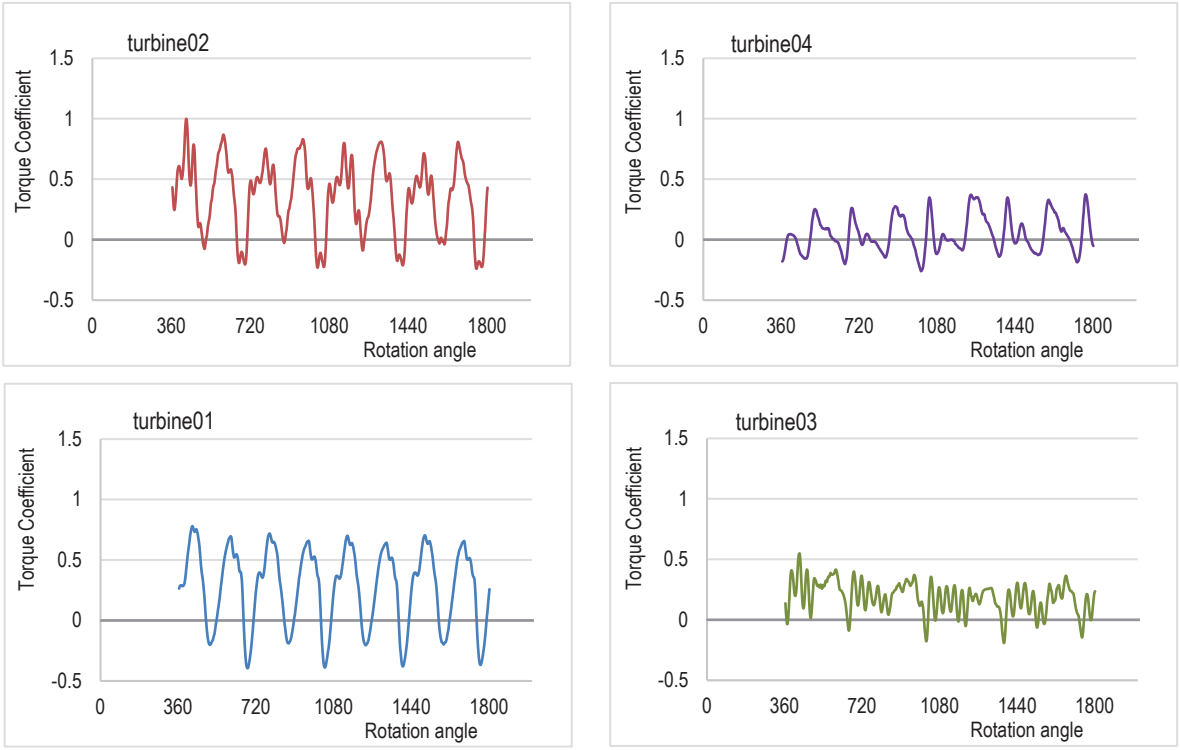

Fig.11 Time history of the torque coefficient (0 degrees flow)

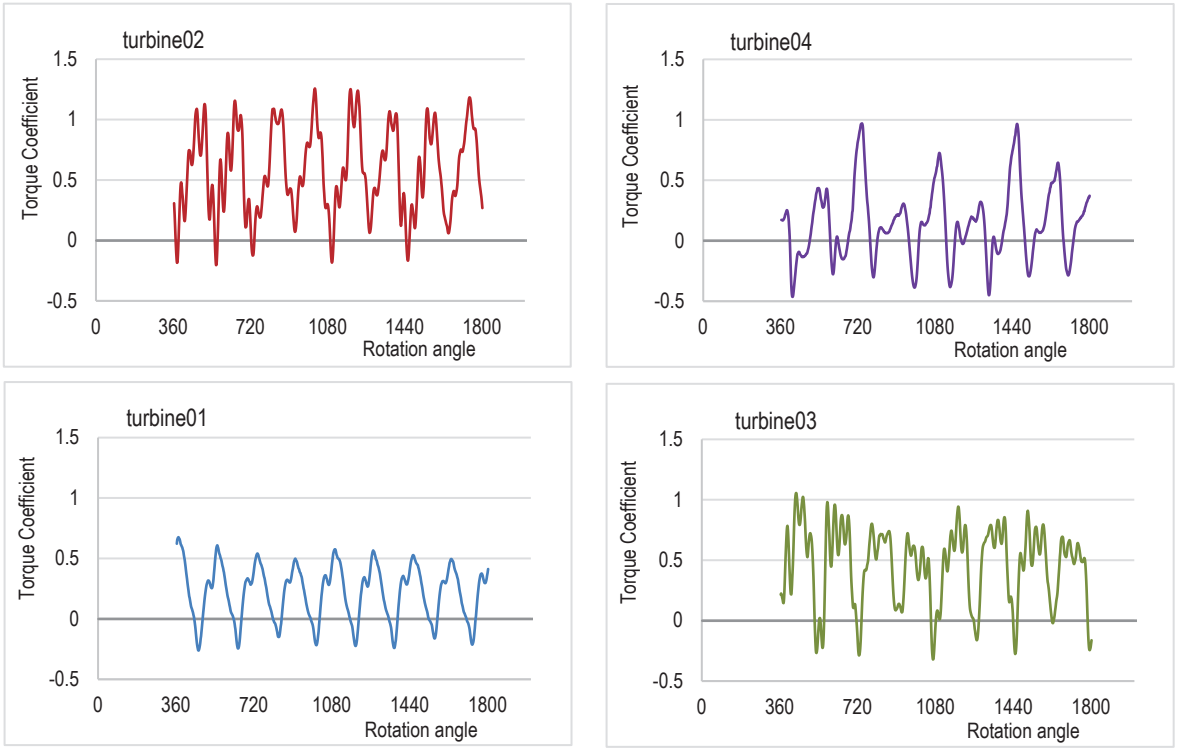

Fig.12 Time history of the torque coefficient (45 degrees flow)

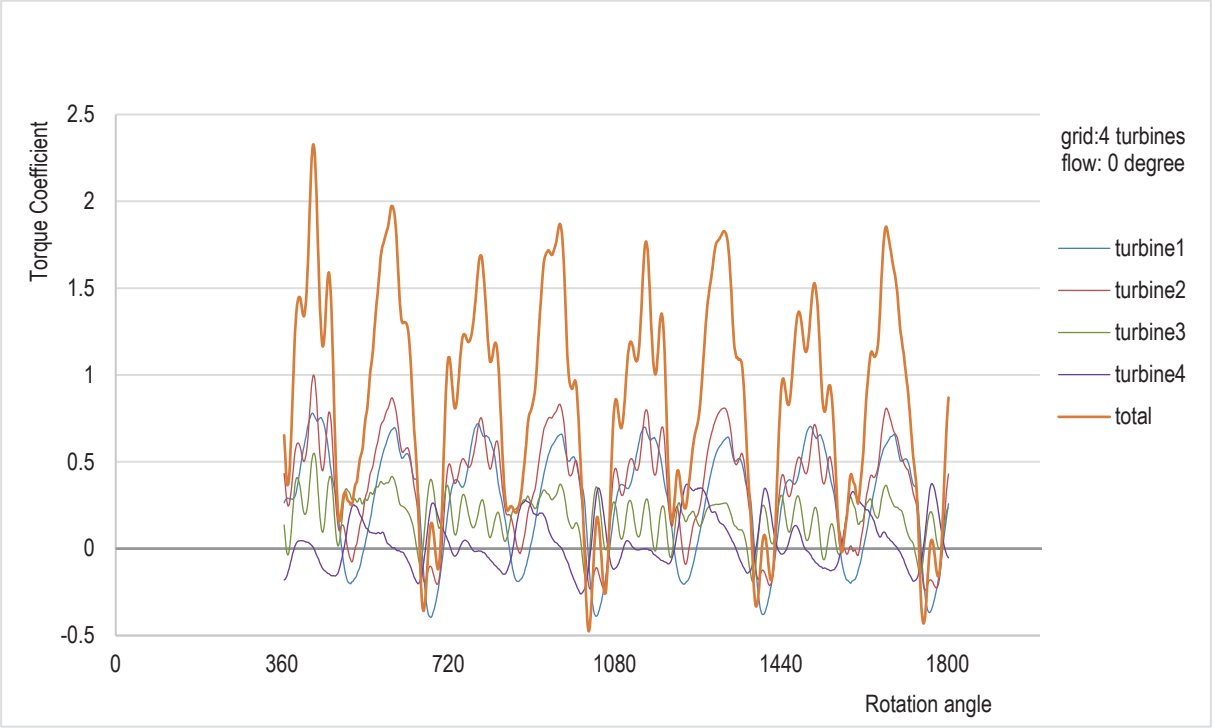

Fig.13 Time history of the torque coefficient (0 degrees flow)

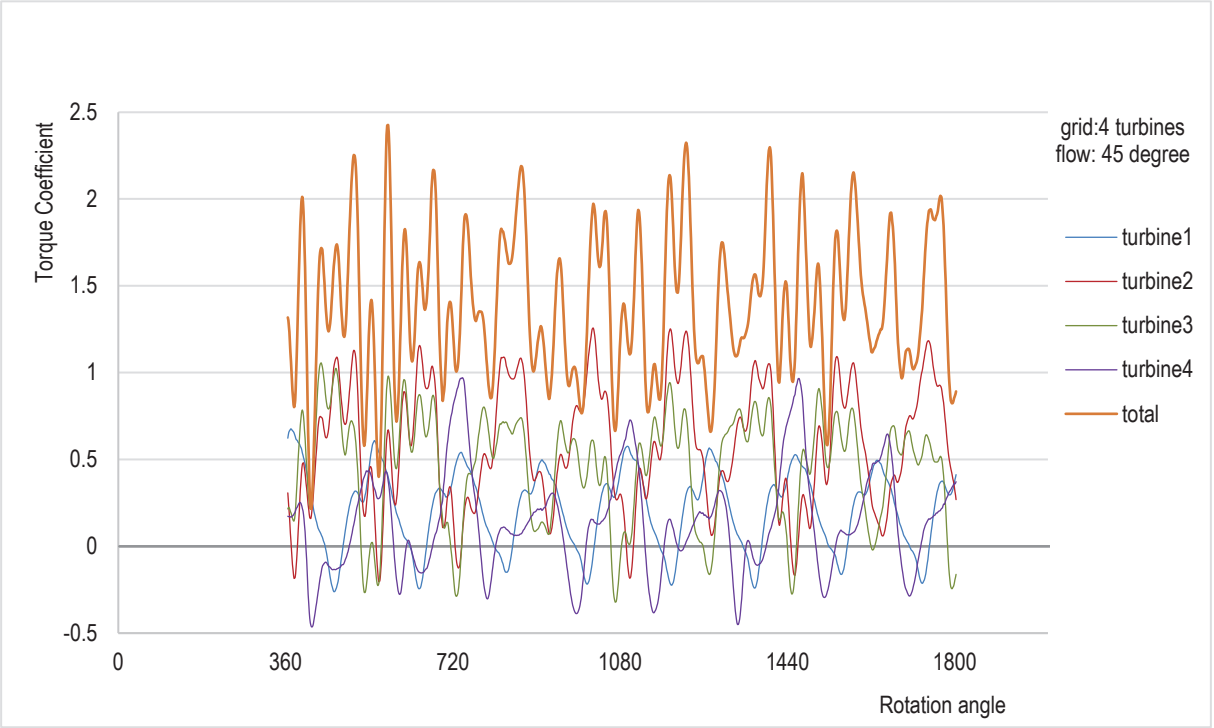

Fig.14 Time history of the torque coefficient (45 degrees flow)

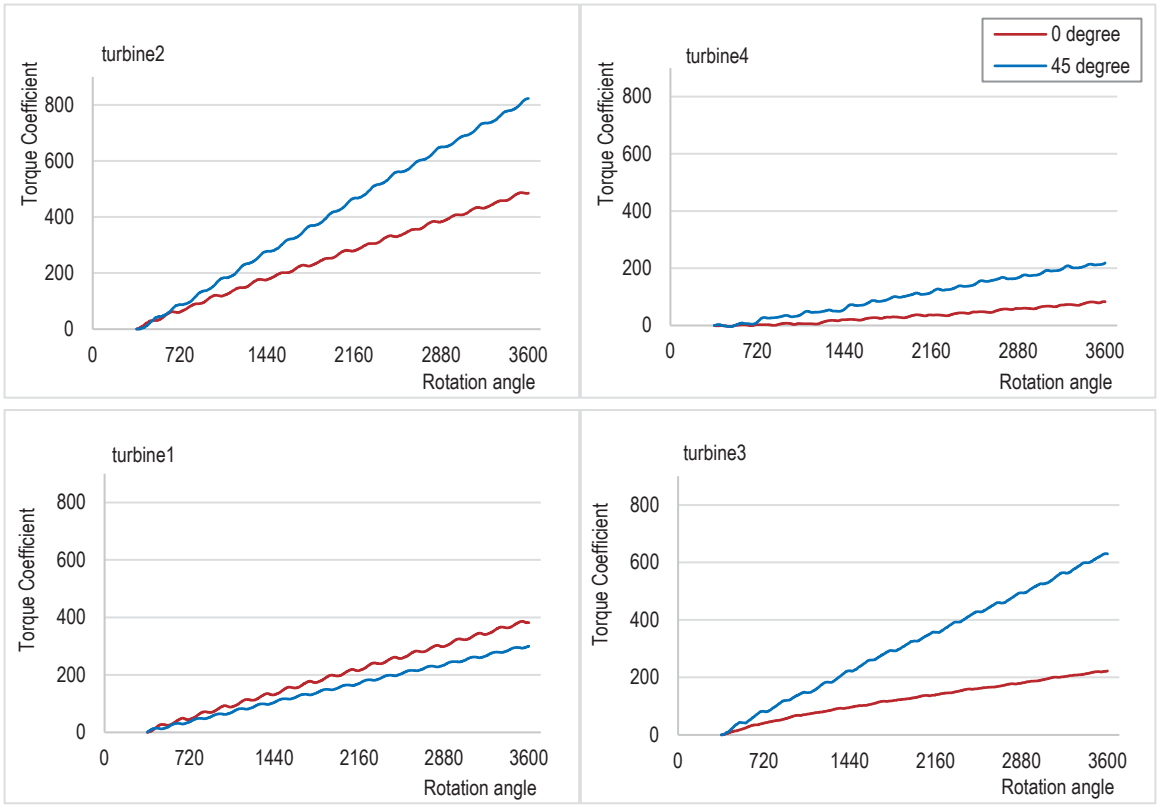

Fig.15 Total value of the torque coefficient

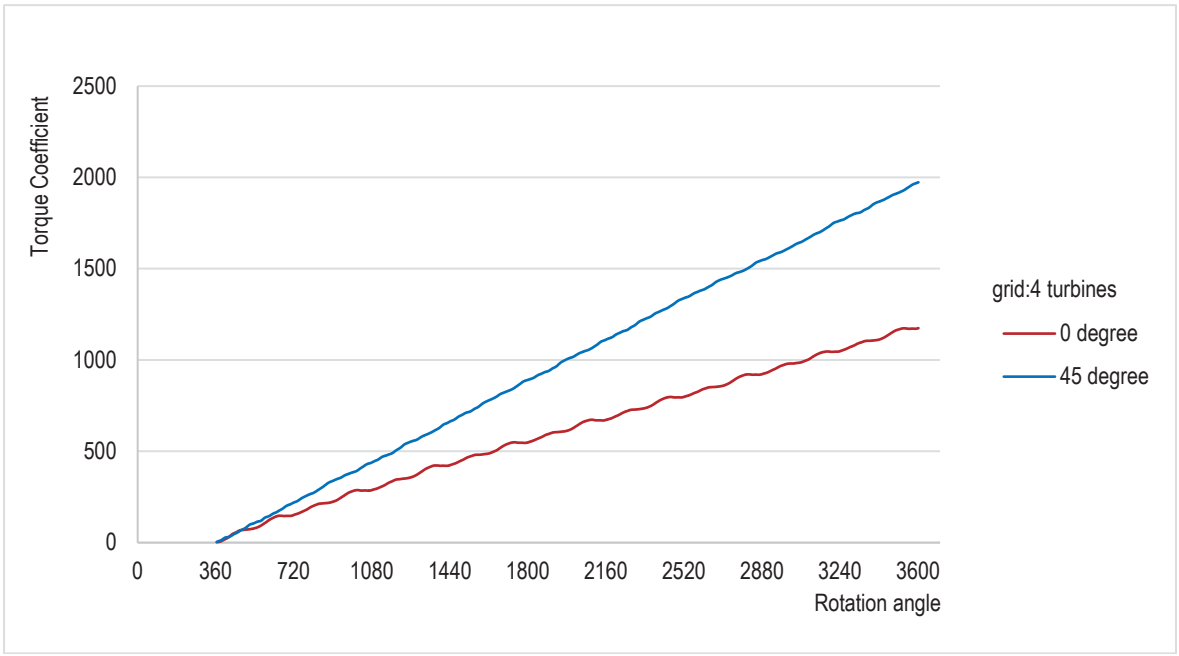

Fig.16 Total value of the torque coefficient of four turbines

5. SUMMARY

A two-dimensional simulation was performed for four independently rotating vertical axis Savonius turbines and the effect of interaction was investigated by changing the angle with the mainstream.

In order to rotate multiple devices, the flow region was divided into a region close to each rotating device and a non-rotating region outside. Then, we used a method to accurately connect each joint at the boundary of each region. In addition, the region inside the Savonius turbine is divided into the blade region where the flow flows in and out and the overlapping region. As a result, it was possible to analyse the flow passing through the overlapped gap. When the direction of the mainstream was changed with respect to the line connecting the rotating shafts of the turbines, it was observed that a complicated flow was generated due to the positional relationship of the four turbines. It was also observed that when the angle of attack of the mainstream is 45 degrees, the change in the flow caused by the upstream turbine affects the downstream turbine. These flow characteristics can be understood to some extent from the relationship between the direction of the mainstream and the direction of rotation of the turbine.

Investigating the torque value of each turbine and the total torque value of all turbines, it is found that when the mainstream angle of attack is 45 degrees, the value is about 68% larger than when it is 0 degrees. This means that the torque can be effectively obtained through the interaction between the mainstream direction and the device

Future tasks include investigating the interaction when the distance between the turbines is varied, and investigating the case where the number of turbines is further increased to examine the layout of the entire ocean current power generation system.

References

[1] Ogawa, T., Yoshida, H. and Sugiura, S., “Study of a Savonius-Type Wind Turbine (4th Report, Effects of the Mutual Interaction)”, Transaction of the Japan Society of Mechanical Engineers Series B, Vol 52, No.481(1986)

[2] Minakawa, A. and Kawamura, T., “Numerical simulation of interaction between two Savonius turbines aimed at practical application of ocean current power generation”, WCCM - APCOM 2022, Volume 600 Fluid Dynamics and Transport Phenomena, DOI: 10.23967/wccm-apcom.2022.084 (2022)

[3] Kawamura, T., “Introduction to numerical simulation”, Computer Science Library 17 Saiensu-sha (2006)

[4] Ishimatsu, K., Shinohara, T and Takuma, F., “Numerical Simulation for Savonius Rotors”, Transactions of the Japan Society of Mechanical Engineers B, Vol.69, No.569 (1994)

[5] Yanenko, N. N., “The method of fractional steps”, Springer Springer-Velag, (1971)

[6] T. Kawamura and K. Kuwahara, “Computation of high Reynolds number flow around a circular cylinder with surface roughness”, AIAA Paper, 84 84-0340 (1984)

Akiko Minakawa
Department of Computer Science, Graduate School of Humanities and Sciences, Ochanomizu University
2-1-1 Otsuka, Bunkyo-ku, Tokyo, 112-8610, Japan
E-mail: minakawa.akiko@is.ocha.ac.jp

Tetuya Kawamura
2-1-1 Otsuka, Bunkyo-ku, Tokyo, 112-8610, Japan
E-mail: kawamura@is.ocha.ac.jp